Top quark resonances in ATLAS simulation

DESY Summer Student Programme, 2012

Stefanie Todt
TU Dresden, Germany

Supervisor
Elin Bergeaas Kuutmann

31th of August 2012

Abstract

This report presents a study on the reconstruction of top/anti top quark resonances. Three selection methods for events with low (resolved) and very high (boosted) invariant masses are investigated with special emphasis on highly boosted systems. Reconstruction properties of the decay of $t\bar{t}$ pairs originating from a hypothetical, heavy particle, called Z', are compared to Standard Model top pair decays. A novel variable for lepton isolation, called mini-isolation, is applied as a selection criterion for leptons, in order to improve signal efficiencies with respect to standard isolation variables. Additionally the application of jet trimming on large-radius jets is investigated, which mainly reduces the impact of high luminosity effects at the LHC.

TECHNISCHE UNIVERSITÄT DRESDEN

DESY

Contents

1 Introduction

This report studies $t\bar{t}$ resonances which are produced by hypothetical heavy particles in the mass range of TeV decaying into a pair of top (t) and anti-top ($\bar{t}$) quarks. Since the Standard Model does not contain any elementary particle which is heavier than a top quark ($m_t \approx 173$ GeV [1]) and therefore cannot decay into $t\bar{t}$ pairs these studies provide an approach to new physics beyond the Standard Model. The model which is discussed in this analysis is a new gauge boson Z' which has the same properties as the known Z boson but has a much higher mass [2, 3].

A top quark promptly decays into a b quark and a W boson which itself decays either hadronically or leptonically. This analysis studies the case where the W boson originating from one of the (anti)top quarks decays into a charged lepton and the corresponding neutrino and the other into a pair of light quarks (called semileptonic top/anti top quark decay). All quarks then form jets in the detector.

Standard Model top pairs are mainly produced with an invariant mass close to the mass sum of both top quarks and only a minority of events reaches very high energy ranges. In the lower energy ranges the decay products are well separated in the detector which gives a resolved signature where the decay products can be reconstructed separately. If, however, the top/anti-top pair originates from the decay of the heavy Z' their decay products are always highly boosted leaving a signature in the detector where they are very close together or overlap each other and therefore cannot be detected separately.

This report investigates reconstruction methods for the resolved and boosted events, aiming to improve the selection criteria for the boosted case in order to gain a better signal to SM-$t\bar{t}$ background discrimination. A detailed analysis concentrates on the isolation criteria for the lepton related to the nearby b quark jet in the boosted case. A new isolation algorithm, called mini-isolation, is compared to standard fixed cone isolation variables[1]. Furthermore the substructure of the fat merged jet in boosted events originating from the overlapping of the two jets from the hadronically decaying W and the b quark jet is investigated. Therefore the impact of "jet grooming", in particular jet trimming, on the boosted event reconstruction is studied.

Within these studies Monte-Carlo (MC) generated samples for $t\bar{t}$ background and Z' production are used[2].

In the following section the LHC and in particular the ATLAS experiment are introduced. Section 3 explains how the event selection for the different cases is done. Additionally it gives a short description of the used variables for lepton isolation and jet trimming. The procedure of event reconstruction is explained in Section 4 and Section 5 studies the impact of the application of the different variables on the invariant mass of the $t\bar{t}$ system.

2 LHC and ATLAS

2.1 The LHC

The LHC (**L**arge **H**adron **C**ollider) is a particle accelerator situated at CERN near Geneva on the border between Switzerland and France. It provides the worlds biggest physics instrument in order to study elementary particles in an unprecedented energy range. It is

[1] For mini-isolation MiniIsolation10 and for the standard isolation Ptcone30 and Etcone20 are used.

[2] For $t\bar{t}$ using MC@NLO [4, 5] with shower generator HERWIG [6, 7] and JIMMY [8] and for Z' using PYTHIA [9]. For ATLAS detector simulation GEANT4 [10] was used.

built 100 m underground for cosmic radiation background rejection. The LHC is a proton-proton collider currently operating at a center-of-mass energy of 8 TeV. Since protons are not elementary particles but instead consist of quarks and gluons (called partons) the actual interaction happens between the partons inside the protons. The collider has two beam pipes, one for each of the two proton beams traveling in opposite directions. Each proton beam is divided into several bunches which are separated by 25 ns and contain about 10^{11} protons each. At design luminosity about 20 collisions per bunch crossing take place, but only very few interaction are of physics interest. This phenomenon is called "pile up" and physics analysis has to deal with it since every event is a superposition of several parton-parton collisions. It is hard to determine the original interaction point for every particle under such conditions since the partons hadronise because of colour confinement in strong interactions and form showers of many hadrons.

At LHC there are mainly four experiments: ALICE, ATLAS, CMS and LHCb. In this study, simulations of interactions in ATLAS are used. The ATLAS detector is described in the next section.

2.2 The ATLAS detector

ATLAS (**A** **T**oroidal **L**HC **A**pparatu**S**) is a general-purpose detector for high energy physics [11]. In figure 1 a scheme of the ATLAS detector is shown.

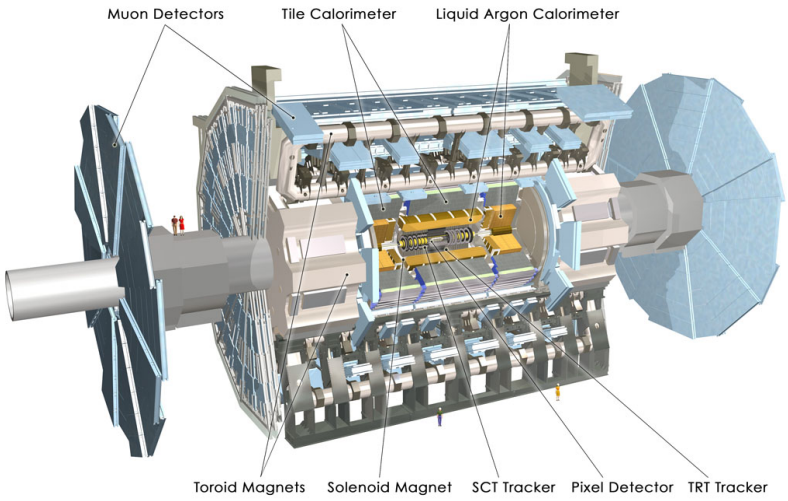

Figure 1: The ATLAS detector (Image from atlas.ch)

It has a barrel region, which is built up in several concentric layers around the beam pipe, and two end cap regions perpendicular to the beam pipe. The whole detector consists of four major components: the inner detector, the calorimeters, the muon spectrometer and the magnet system.

The inner detector traces the tracks which charged particles leave when interacting with the detector material. Since the particles interact via ionization only the tracking of charged particles is possible. It contains a high-resolution pixel detector at its innermost layer, a semiconductor tracker (SCT) in the middle layer, and a transition radiation tracker (TRT) at the outermost layer. All components are enclosed by a magnetic field which allows to measure the particle momentum and to determine the particle charge using the

curvature of its track (Lorentz force). Although the TRT is not as precise as the other two detectors it has the capability to significantly distinguish between electrons and other (heavier) particles. Additionally by following the tracks of the particles to their origin it is possible to reconstruct the interaction point (vertex).

The calorimeters measure the energy of the particles through total absorption. Electrons and photons form electromagnetic showers mostly in the electromagnetic calorimeter. Hadrons propagate further causing more wide-spread hadronic showers mainly in the denser hadronic calorimeter. Unlike the tracking detectors the calorimeters can also detect neutral particles.

The outermost detector parts are the muon chambers. Since muons are leptons, like electrons, but 200 times heavier they travel through all the previous detector layers only losing a small amount of energy through ionization. The muon chambers are surrounded by large toroid magnets for high precision measurements of the muons momentum.

In order to handle the huge amount of data a trigger system is implemented in the data taking process. It is divided into three levels. The first-level trigger analyzes information from the calorimeters and the muon chambers. It keeps the interesting events and passes the regions of interest to the second-level trigger. The third trigger level, called event filter, then does a more detailed investigation of these regions of interests. The whole trigger system reduces the event rate from 40 million per second at the beginning to 300.

The ATLAS coordinate system is briefly introduced here since it will be used throughout this report. The interaction point of interest (nominal vertex) is chosen as the origin of a right-handed coordinate system. The beam pipe defines the z-axis and the x-y plane forms the transverse plane which lies perpendicular to the beam pipe providing the azimuthal angle ϕ. θ defines the angle between the measured particle and the positive z-axis. The rapidity is defined as:

$$y = \frac{1}{2} \ln \left[\frac{E + p_z}{E - p_z} \right]$$

which has the essential properties of being invariant to Lorentz boosts. In the limit of massless particles the rapidity is equal to the geometrically defined pseudorapidity η:

$$\eta = -\ln \tan \left(\frac{\theta}{2} \right)$$

Since mainly all particles can be considered massless in respect to the nominal center-of-mass energy the pseudorapidity is a good approximation of y. An angular distance can then be defined through the distance parameter:

$$\Delta R = \sqrt{(\Delta\eta)^2 + (\Delta\phi)^2}$$

The transverse momentum p_T, the transverse energy E_T and the missing transverse energy E_T^{miss} are defined in the x-y plane.

3 Event selection

Top quarks have a very short lifetime ($\tau \approx 10^{-25}$ s) compared to the timescale for strong interactions [12]. Therefore they do not form hadrons like the other quarks, but decay via the weak force. Top quarks are only detected via their weak decay into a W boson and a

b quark in most of the cases (99, 8% [1]).

This analysis considers only semileptonic $t\bar{t}$ decay processes (Figure 2(a)). This leads to events where a charged lepton and its neutrino (from the leptonic W decay), and one b jet is produced in one (anti)top decay and the other (anti)top decay produces two light quark jets (from the hadronic W decay) and one b jet. Only electrons and muons are included in the analysis since tau leptons decay mainly and quickly into hadrons. Only the leptonical decay of the τ is counted via the resulting electrons or muons. Neutrinos do not interact with the detector material and therefore cannot be detected directly but they carry away a certain amount of momentum and energy. This amount can be calculated through energy and momentum conservation. But since the exact initial energy/momentum in the direction of the beam collision is unknown, energy conservation can only be considered in the transverse plane to the beam. Neutrinos then are associated with the missing transverse energy E_T^{miss} in an event. Semileptonic events are chosen for analysis because events with jets only are hard to reconstruct and suffer from huge QCD background. Events with two charged leptons have also two neutrinos both carrying away transverse energy. But as only the sum of this missing E_T is known, the information about the direction and energy of each single neutrino is lost.

3.1 Object definitions and Common event selection

All physics objects used to reconstruct an event have to follow certain object definitions and the whole event has to pass quality requirements for the measurements of the different detectors. Electrons, muons and jets measurements have for example restrictions on their pseudorapidity η (defined in Section 2.2) to make sure that they lie within the acceptance of the detector and trigger mechanism. Furthermore the lepton has to be isolated from jets to increase the reliability on the lepton reconstruction from the detector measurements and to make sure that the energy deposits in the calorimeters are not counted twice. The different isolation methods are discussed in detail in Section 3.4. Jets are reconstructed from the energy deposition in the hadronic calorimeter with the inclusive anti-k_t [13] jet finding algorithm. These algorithms then define jets with a certain radius parameter (similar to the radius of a $\eta-\phi$-cone). Normal jets occurring in resolved events are defined by a radius parameter $R = 0.4$.

After passing these quality requirements which define good objects, common event selection cuts are applied which are used for both the resolved and boosted analysis to increase the $t\bar{t}$ signal fraction. Since only semileptonic events shall be considered there has to be at least one good electron (muon) with a transverse energy E_T (momentum p_T) higher than 25 GeV. Furthermore the event should not display a second good electron (muon) with $E_T > 25$ GeV ($p_T > 20$ GeV) but can contain leptons with lower E_T/p_T. The missing transverse momentum E_T^{miss} is required to be larger than 30 GeV for electron events (larger than 20 GeV for muon events) to count for a high energetic neutrino. The transverse mass $M_T = \sqrt{(E_T^{lepton} + E_T^{miss})^2 - (p_T^{lepton} + p_T^{miss})^2}$ of the lepton + E_T^{miss} system which is related to the transverse mass of the leptonically decaying W boson has to fulfill $M_T > 30$ GeV in the electron channel and $M_T + E_T^{\text{miss}} > 60$ GeV in the muon channel.

After this common selection, specific selection cuts according to resolved or boosted analysis are applied, as described in the following sections.

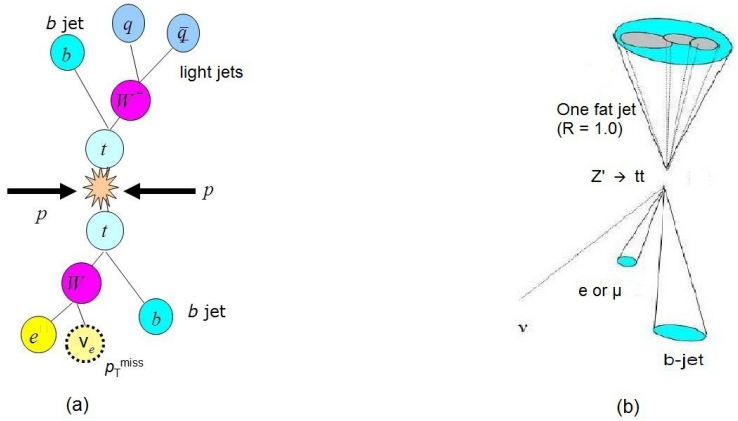

Figure 2: (a) Scheme of a pp collision producing a $t\bar{t}$ pair which decays semileptonically (b) Scheme of the boosted event selection where $t\bar{t}$ pair originates from a Z'

3.2 Resolved event selection

In Standard Model events the $t\bar{t}$ pair decays almost at rest. Therefore the four jets from this decay are well separated and the angular distribution of the different (anti)top decay products are unrelated to each other. This leads to the requirement to have at least four good jets ($R = 0.4$) with transverse momentum $p_T^{jet} > 25$ GeV. In some cases two jets have already merged to one bigger jet revealing a slightly boosted top quark pair. In this case the selected event has to contain at least 3 jets of $R = 0.4$, $j_{0.4}$ where one of these jets has transverse mass $m_{j_{0.4}}$ bigger than 60 GeV. The transverse mass of a jets in obtained by summing over the energy-momentum four vectors of all jet constituents:

$$m_j = \sqrt{\left(\sum_i E_i\right)^2 - \left(\sum_i p_i\right)^2}$$

In both cases one of these jets has to originate from a b quark which is proved by special algorithms for "b-tagging".

3.3 Boosted event selection

A schematic view of a boosted $t\bar{t}$ decay from a Z' is shown in figure 2(b). The massive Z' decays at rest. For this reason the top quarks of the $t\bar{t}$ pair are sent out in opposite direction to each other having a very high transverse momentum in their direction of flight. This leads to highly collimated decay products which have a very high p_T because of the large invariant mass of the Z'. Therefore the hadronically decaying top quark is reconstructed as one fat jet with radius parameter $R = 1.0$, $j_{1.0}$. Since this jet should contain three jets its mass and substructure has to be investigated. For the jet mass $m_{j_{1.0}}$ a lower limit of 100 GeV is set while $p_T > 350$ GeV. For substructure studies the variable $\sqrt{d_{12}}$ is used which is related to the mass splitting of the two highest p_T subjets which have merged in this fat jet [14]. If the $R = 1.0$ jet contains constituents of a two body decay (like for $t \to Wb$) the mass splitting for the highest p_T subjets is expected to be half the mass of the originating particle, in the $t\bar{t}$ case $\sqrt{d_{12}} \approx m_t/2 \approx 85$ GeV. Therefore a cut on $\sqrt{d_{12}} > 40$ GeV is applied. Additionally to one fat jet, one jet with $R = 0.4$ has to meet the same selection

requirements like in the resolved case.

Due to the back-to-back structure of the event the decay products show relations between their angular distribution. Hence, cuts that pay attention to this can be applied. The closest small jet to the lepton is considered as the lepton jet j_l. Moreover the fat jet is required to have a large azimuthal distance to the lepton $\Delta\phi(lepton, j_{1.0}) > 2.3$ and also a large transverse distance to the lepton jet $\Delta R(j_l, j_{1.0}) > 1.5$.

Here again any of the small jets in the event has to be b-tagged.

3.4 Lepton isolation

Selected events are required to have at least one isolated lepton. An isolated lepton is expected for decays when the (anti)top quark pair is created at rest. In this case the standard relative isolation criteria for leptons is used which count up the energy deposited in a fixed cone around the lepton [15, 16]. Since, however, the decay products originating from one of the tops in a boosted configuration are highly collimated, the lepton and the accompanying b jet from the leptonically decaying W boson will often overlap or at least occur in a narrow cone close together. In order to reject background from light QCD jets with embedded hard leptons when applying no isolation, but meanwhile keep high signal efficiencies, the normal isolation criteria has to be modified. The so called mini-isolation [17, 18], is defined through a cone which depends on the lepton p_T:

$$\Delta R(lepton, track) = \frac{10GeV}{p_T^l}$$

All tracks which have $p_T^{track} > 1.0$ GeV and lie within this cone (except the lepton track) are added up forming the mini-isolation variable I_{mini}^l. This variable is then divided by the lepton p_T and has to meet an upper limit for selection. With this isolation criterion the separation between the lepton and the b jet scales inversely with the lepton p_T leading to that softer leptons has to be more isolated that harder leptons.

3.5 Jet trimming

Due to the high-luminosity conditions at the LHC hard-scatter processes are always accompanied by soft-scatter interactions like pile-up (Section 2.1) as well as initial- and final-state radiation. Particularly large jets with $R = 1.0$ suffer from this contamination since they cover a wide area of the detector. This leads to difficulties to resolve the particles in the jet, which come from the hard interaction and therefore the mass resolution in boosted topologies, where one large jet contains all decay products, is diminished.

The jet trimming algorithm [14] reduces the influence of these soft contributions in large jets using of the structural differences (like the splitting variable $\sqrt{d_{12}}$ introduced in Section 3.3) between jets formed from light quarks or gluons and large jets which contain boosted decay products. It takes advantage of the fact that those contaminations mentioned above are often much softer than the contributions of the hard-scatter partons.

The algorithm proceeds by reclustering the jet with the inclusive k_t algorithm [19], [20] to create subjets of a radius parameter R_{sub} from the original jet. It removes subjets with $p_T^i/p_T^{jet} < f_{cut}$ where p_T^i is the transverse momentum of the subjet, p_T^{jet} the initial large jet p_T and f_{cut} the algorithm parameter. The remaining subjets form the trimmed jet.

This process retains the characteristic substructure within the jet while mitigating the influence of soft radiation.

4 Event reconstruction

The aim of the event reconstruction is to calculate the invariant mass of the $t\bar{t}$ system which is determined by the selected objects.

For both the resolved and boosted selection, the longitudinal momentum p_z from the neutrino is added to the reconstruction procedure. It is calculated by assuming that the main part of the missing transverse energy comes from the neutrino and the W boson indeed decayed into the selected charged lepton and a neutrino [21].

For the resolved selection the simplest approach, of just adding up the four vectors of the four highest p_T jets, the charged lepton and the neutrino, is extended to a method, called dRmin algorithm [16]. This method aims to identify the jets originating from the $t\bar{t}$ decay while rejecting jets which stem from initial or final state radiations, and thereby improving the mass resolution of the reconstruction. It starts to treat the four jets with the highest p_T but excludes one, if it meets the requirement ΔR(jet, lepton/closest jet) $> 2.5 - 0.015 \cdot m_j$[GeV] for the angular separation between the chosen jet and the lepton or the closest jet. This results in discarding a jet, if it is too far away from other jet clusters. This procedure is iterated if more than 3 jets remain. These remaining jets together with the charged lepton and the neutrino are then used to reconstruct the $t\bar{t}$ invariant mass.

If, in the resolved selection, there exists a jet with mass higher than 60 GeV, this jet is considered to originate from the hadronic W decay. Then this jet together with its closest jet form one top quark decay while the leptonically decaying W (from the charged lepton and the neutrino) and the closest jet to it are combined to form the other top quark decay products.

In boosted event reconstructions simply the four-vectors of the remaining highest p_T jet with $R = 1.0$, the $R = 0.4$ lepton jet (closest jet to the lepton), the selected lepton and the neutrino are summed up to form the invariant system.

5 Results

5.1 Comparison of Z' and $t\bar{t}$ MC-simulated data

The distribution of the reconstructed invariant $t\bar{t}$ mass for resolved and boosted reconstruction are compared. All Monte Carlo samples are reweighted such that they agree with data distributions[3]. For the Z' a mass of $m_{Z'} = 1600$ GeV is chosen. The cross section for Z' multiplied by the branching ratio[4] for the decay $Z' \to t\bar{t}$ for the chosen Z' mass is 0.09 pb [2, 3] whereas for the semileptonic decay of Standard Model $t\bar{t}$ background it is 90.55 pb [22][5]. As this gives a difference of three orders of magnitude between these values, the shown histograms are not normalized to the cross section unlike conventionally done. In order to compare them, both Z' and $t\bar{t}$ background distributions are each normalized to unity instead. Furthermore the electron and muon channel are treated separately.

Figure 3(a) shows the invariant mass of the resolved selection combining the 3 and 4 jet reconstruction method. In both distributions a peak around the invariant mass of the

[3]The following weights were applied: MC, pile-up, electron and muon scale, btag scale and jet vertex factor scale.

[4]The branching ratio gives the fraction of cases among all other decay possibilities where the Z' decays into a pair of top and anti top quark.

[5]These values for the cross sections are multiplied with a K-factor to contribute to higher-order QCD corrections.

originating particle(s) can be observed. For Z' the mass resolution is worse compared to $t\bar{t}$ because of a long tail towards lower invariant masses. The boundary for $t\bar{t}$ pair production at twice the top quark mass ($2 \cdot m_t \approx 350$ GeV) is clearly visible whereas the number of events steeply falls towards higher invariant masses.

For boosted configurations (see figure 3(b)) the two peaks are less separated due to the selection of boosted contributions of the $t\bar{t}$ background.

Although the boosted event selection in total picks up less events for Z' and $t\bar{t}$ (as shown in table 1), it increases the fraction of signal to background events

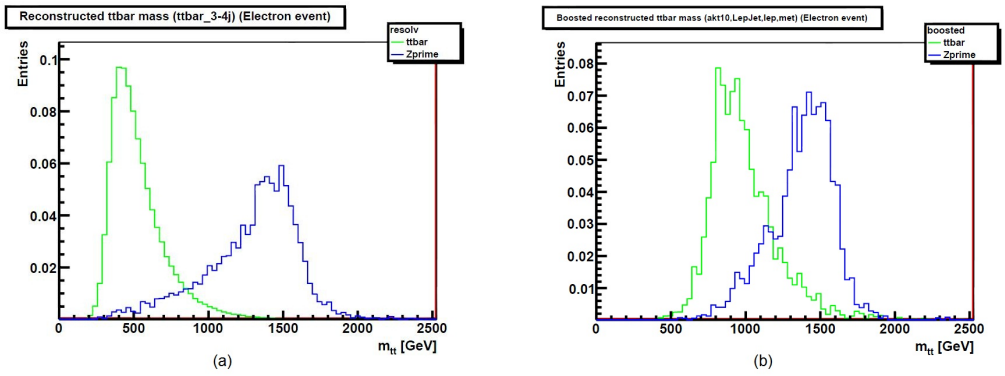

Figure 3: Reconstructed invariant mass m_{tt} of the top/anti top pair for resolved (a) and boosted (b) event selections (electron channel). Both Z' (in blue) and $t\bar{t}$ (in green) distributions are normalized to unity each. For the resolved event reconstruction 3 and 4 jet reconstruction methods are combined. Comparable distributions result in the muon channel (not shown).

	$t\bar{t}$		Z'	
Channel	Electrons	Muons	Electrons	Muons
resolved (mini-isolation)	3,29 %	4,04 %	4,70 %	4,91 %
boosted (trimmed, mini-isolation)	0,02 %	0,02 %	1,4 %	1,8 %

Table 1: Number of selected events for the resolved and boosted event selection with respect to the total number of events before selection cuts were applied.

5.2 Comparison of normal lepton isolation and mini-isolation

In this section two different methods of lepton isolation are compared, the traditionally used fixed cone isolation and mini-isolation.

Figure 4 and 5 show the invariant mass distributions for resolved and boosted selection respectively. For both configurations a similar effect for the Z' signal is observable. Mini-isolation noticeably enhances the number of selected events for electrons (while keeping the same shape compared to normal isolation) whereas for muons only a small effect is visible (table 2). This is due to the already weaker reconstruction requirements for muons because of the fact that they cannot be so easily faked in the detector than electrons. For $t\bar{t}$ the effect for boosted selections is similar while in the resolved case only small differences can be seen. This is because in the resolved event selection, mainly $t\bar{t}$ events with smaller invariant mass are selected. Therefore the lepton is usually more isolated and

the standard fixed cone isolation shows already a good efficiency for those leptons (since is was introduced for these cases).

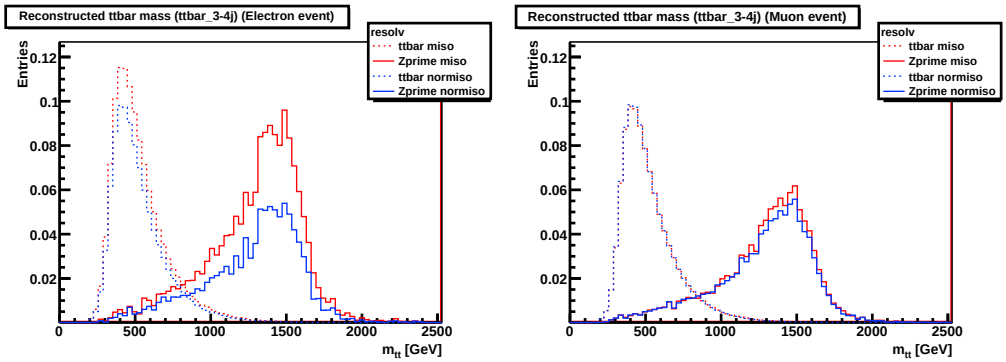

Figure 4: Comparison of fixed cone isolation (in blue) and mini-isolation (in red) for the electron (on the left) and muon (on the right) channel for resolved event selection. Z' (full lines) and $t\bar{t}$ (dashed lines) events are normalized to unity each. The distributions for mini-isolation are normalized with respect to the fixed cone isolation distributions.

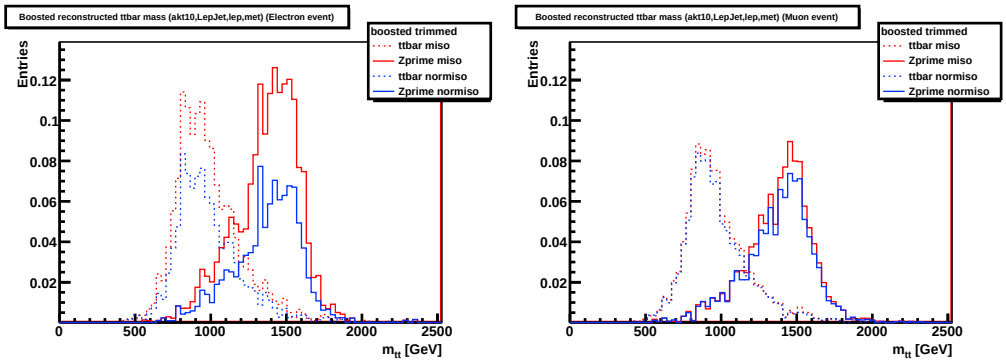

Figure 5: Comparison of fixed cone isolation (in blue) and mini-isolation (in red) for the electron (on the left) and muon (on the right) channel for boosted event selection. Z' (full lines) and $t\bar{t}$ (dashed lines) events with fixed cone isolation are normalized to unity each. The distributions for mini-isolation are normalized with respect to the fixed cone isolation distributions.

5.3 Impact of jet trimming on the invariant mass reconstruction of the ttbar system

In this section the impact of jet trimming on the invariant mass of the fat jet ($R = 1.0$) and the entire $t\bar{t}$ system is investigated. For this analysis the cut parameter on the momentum fraction of the subjets f_{cut} is set to 5% and the subjet radius parameter R_{sub} is fixed at 0.3.

Figure 6 (a) shows the invariant mass of the $R = 1.0$ jet for $t\bar{t}$ and Z' for trimmed and untrimmed jets (with $R = 1.0$). The observation is a slight shift to smaller invariant masses for Z' events. This is due to sorting out subjets with smaller p_T fraction than f_{cut} which then do no longer contribute to the invariant mass of the jet. The mass drop also

	$t\bar{t}$		Z'	
Channel	Electrons	Muons	Electrons	Muons
resolved (mini-isolation)	3,29 %	4,04 %	4,70 %	4,91 %
resolved (standard isolation)	2,77 %	4,05 %	2,89 %	4,91 %
boosted (trimmed, mini-isolation)	0,02 %	0,03 %	1,4 %	1,8 %
boosted (trimmed, standard isolation)	0,01 %	0,03 %	0,80 %	1,63 %

Table 2: Number of selected events for the resolved and boosted event selection for standard and mini-isolation with respect to the total number of events before selection cuts were applied.

leads to a smaller number of selected event since the jets which, before trimming, have a slightly higher mass than the mass cut, fall out of the selection after trimming. This can also be seen in the distribution of the invariant mass (see figure 6 (b)) of the top/anti top system. For the $t\bar{t}$ background the decrease of selected events is about 2 times larger than for Z' (see table 3).

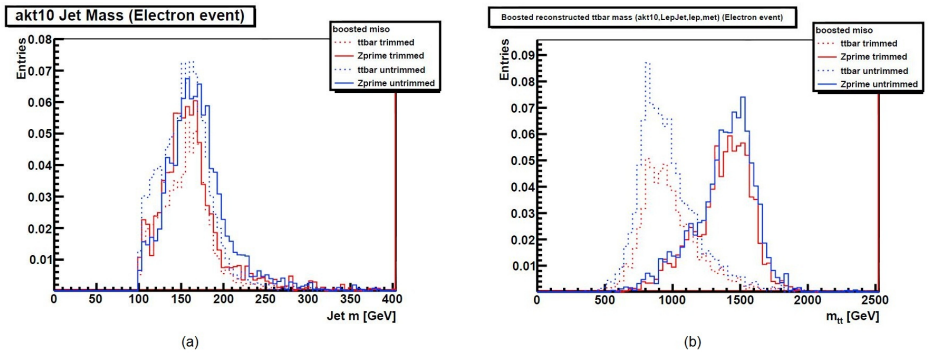

Figure 6: (a) Invariant mass of the jet with radius parameter $R = 1.0$ for boosted selection of Z' (full lines) and $t\bar{t}$ (dashed lines) events in the electron. (b) Reconstructed invariant mass of the top/anti top pair for boosted event selection in the electron (on the right) and muon (on the left) channel for Z' (full lines) and $t\bar{t}$ (dashed lines) events. The trimmed distributions (in red) are normalized with respect to the untrimmed distributions (in blue), which themselves are normalized to unity.

	$t\bar{t}$		Z'	
Channel	Electrons	Muons	Electrons	Muons
boosted (untrimmed, mini-isolation)	0,03 %	0,04 %	1,70 %	2,19 %
boosted (trimmed, mini-isolation)	0,02 %	0,02 %	1,4 %	1,8 %

Table 3: Number of selected events for the resolved and boosted event selection for trimmed and untrimmed large-radius jets with respect to the total number of events before selection cuts were applied.

6 Conclusion

In this report it is demonstrated that the boosted event selection increases the sensitivity to new physics processes with very massive particles. It enhances the signal to background

ratio in the search for the Z'.

It is shown that mini-isolation is an isolation criterion for leptons which works better in boosted environments then the standard isolation. The application of mini-isolation has a noticeable effect on the selection efficiency for electrons. It enhances the number of selected events while keeping the shape of the distribution for the reconstructed invariant mass of the $t\bar{t}$ system. Moreover this effect is larger on the selection of Z' events than on the top/anti top background.

Jet trimming is applied on large-radius jets in boosted topologies in order to reduce the sensitivity to pile-up on the reconstruction of the invariant mass. It shows an enhancement of the signal to background ratio. In total it decreases the number of selected events due to the mass drop effect of trimming and the lower limit cut on large-radius jet mass. This effect, however is lager for the $t\bar{t}$ background leading to an improved selection efficiency for Z'.

Further studies on the impact of mini-isolation and trimming on the event selection both in the resolved and boosted case have to be done by including a more distinguished consideration of the Standard Model background processes.

Acknowledgements

First I want to thank DESY to provide this opportunity to us students to be part of a physicist research team. I would like to thank Karl Jansen for his eagerness and devotion to all the summer students. Thanks also to all people who were involved in the organisation of this summer student programme. I am particularly thankful to Thomas Naumann and the whole ATLAS group for their kindness and sympathy. I am very grateful for the guidance, support and kindness I experienced from my supervisor, Elin Bergeaas Kuutmann, and I would like to thank Thorsten Kuhl, and in particular Christoph Wasicki for his willingness and patience to answer all my questions.

References

[1] Particle Data Group Collaboration, K.Nakamura et al., *Review of particle physics*, J.Phys. **G37** (2010) 075021.

[2] R. M. Harris, C. T. Hill, and S. J. Parke, *Cross section for topcolor Z'(t) decaying to t anti-t*, arXiv:hep-ph/9911288.

[3] R. M. Harris and S. Jain, *Cross Sections for Leptophobic Topcolor Z' decaying to top-antitop*, arXiv:1112.4928 [hep-ph].

[4] S. Frixione and B. R. Webber, *Matching NLO QCD computations and parton shower simulations*, JHEP **06** (2002) 029, arXiv:hep-ph/0204244.

[5] S. Frixione, P. Nason, and B. R. Webber, *Matching NLO QCD and parton showers in heavy flavour production*, JHEP **08** (2003) 007, arXiv:hep-ph/0305252.

[6] G. Corcella et al., *HERWIG 6: Event generator for hadron emission reactions with interfering gluons (including supersymmetric processes)*, JHEP **101** (2001) 10. hep-ph/0011363.

[7] G. Corcella, I. Knowles, G. Marchesini, S. Moretti, K. Odagiri, et al., *HERWIG 6.5 release note*, arXiv:hep-ph/0210213 [hep-ph].

[8] J. M. Butterworth, J. R. Forshaw, and M. H. Seymour, *Multiparton interactions in photoproduction at HERA*, Z. Phys. **C72** (1996) 637–646, arXiv:hep-ph/9601371.

[9] T. Sjostrand, S. Mrenna, and P. Skands, *PYTHIA 6.4 physics and manual*, JHEP **05** (2006) 026, arXiv:hep-ph/0603175.

[10] GEANT4 Collaboration, S. Agostinelli et al., 852 GEANT4: *A simulation toolkit*, Nucl. Instrum. Meth. **A506** (2003) 250–303.

[11] ATLAS Collaboration, G. Aad et al., *The ATLAS Experiment at the CERN Large Hadron Collider*, JINST **3** (2008) S08003.

[12] A. Quadt, *Top quark physics at hadron colliders.* European Physical Journal **C48** (2006).

[13] M. Cacciari, G. P. Salam, and G. Soyez, *The Anti-k(t) jet clustering algorithm*, JHEP **0804** (2008) 063, arXiv:0802.1189 [hep-ph].

[14] ATLAS Collaboration, *Performance of large-R jets and jet substructure reconstruction with the ATLAS detector*, ATLAS-CONF-2012-065, June 2012.

[15] ATLAS Collaboration, *A search for ttbar resonances in lepton+jets events with highly boosted top quarks collected in pp collisions at* $\sqrt{s} = 7$ *TeV with the ATLAS detector*, submitted to JHEP (2012), arXiv:1207.2409v1 [hep-ex].

[16] ATLAS Collaboration, *A search for ttbar resonances with the ATLAS detector in* $2.05 fb^{-1}$ *of proton-proton collisions at* $\sqrt{s} = 7$ *TeV*, Eur.Phys.J. **C72** (2012) 2083, arXiv:1205.5371v3 [hep-ex].

[17] ATLAS Collaboration, *Prospects for top anti-top resonance searches using early ATLAS data*, ATLAS public note, ATL-PHYS-PUB-2010-008, Jul, 2010.

[18] K. Rehermann and B. Tweedie, *Efficient Identification of Boosted Semileptonic Top Quarks at the LHC*, JHEP **1103** (2011) 059, arXiv:1007.2221 [hep-ph].

[19] S. D. Ellis and D. E. Soper, *Successive combination jet algorithm for hadron collisions*, Phys. Rev. **D48** (1993) 3160, arXiv:hep-ph/9305266 [hep-ph].

[20] S. Catani, Y. L. Dokshitzer, M. Seymour, and B. Webber, *Longitudinally invariant* k_t *clustering algorithms for hadron hadron collisions*, Nucl. Phys. **B406** (1993) 187.

[21] T. Chwalek, *Messung der W-Boson-Helizittsanteile in Top-Quark-Zerfällen mit dem CDF II Experiment und Studien zu einer frühen Messung des ttbar-Wirkungsquerschnitts mit dem CMS Experiment.* PhD thesis, Karlsruhe, U., Karlsruhe, 2010. http://cdsweb.cern.ch/record/1416031. Presented 12 Feb 2010.

[22] M. Aliev, H. Lacker, U. Langenfeld, S. Moch, P. Uwer, et al., *HATHOR: HAdronic Top and Heavy quarks crOss section calculatoR*, Comput.Phys.Commun. **182** (2011) 10341046, arXiv:1007.1327 [hep-ph].